Dalton Transactions

ROYAL SOCIETY OF CHEMISTRY

COMMUNICATION

View Article Online
View Journal | View Issue

Cite this: *Dalton Trans.*, 2022, **51**, 13606

Received 6th July 2022,
Accepted 28th August 2022

DOI: 10.1039/d2dt02178a

rsc.li/dalton

Parahydrogen-induced polarization study of imine hydrogenations mediated by a metal-free catalyst†

Danila O. Zakharov, [a] Konstantin Chernichenko,‡[b] Kristina Sorochkina,[a,b] Timo Repo [b] and Vladimir V. Zhivonitko *[a]

Parahydrogen-induced polarization is a nuclear spin hyperpolarization technique that can provide strongly enhanced NMR signals for catalytic hydrogenation reaction products and intermediates. Among other matters, this can be employed to study the mechanisms of the corresponding chemical transformations. Commonly, noble metal complexes are used for reactions with parahydrogen. Herein, we present a PHIP study of metal-free imine hydrogenations catalyzed by the *ansa*-aminoborane catalyst QCAT. We discuss the reaction mechanism by showing the pairwise nature of the initial hydrogen activation step that leads to the formation of the negative net nuclear spin polarization of N–H hydrogen in the QCAT-H_2 intermediate, enabling the further transfer of parahydrogen-originating protons to the imine substrate with the accumulation of hyperpolarized amine products. Parahydrogen-induced polarization also demonstrates the reversibility of the catalytic cycle.

Introduction

Amines are an important class of compounds widely used in various crucial areas such as the food, agrochemical and pharmaceutical industries.[1,2] There are several synthetic methods employed to produce amines, among which metal-catalyzed reductions of imines, enamines, and nitriles are the most important ones.[3] These approaches, however, use costly noble metals and can produce toxic chemical wastes.[4] As an alternative, metal-free reductions of imines are known, such as those with hydroborate reagents.[5] Other reported methods include Brønsted acid-catalyzed reduction with Hantzsch esters as the hydrogen source,[6,7] Lewis base-catalyzed hydrosilylation with trichlorosilane[8,9] and intermolecular hydroamination.[10] In addition, hydrogenations of imines and enamines using frustrated Lewis pairs (FLPs) — pairs of sterically hindered Lewis acids and bases — were reported.[11–13] In these reactions, derivatives of $B(C_6F_5)_3$ are typically involved as Lewis acids forming intermolecular FLPs with the nitrogen-containing reagents. FLPs and molecular hydrogen generate hydroborates *in situ* as active catalytic species, thus bridging the gap between traditional metal-catalyzed hydrogenations and hydroborate reducing agents. In 2008, it was shown that the intramolecular FLP 1-{2-[bis(pentafluorophenyl)boryl]benzyl}-2,2,6,6-tetramethylpiperidine, CAT (Scheme 1), can catalyze the hydrogenation of imines and enamines by molecular hydrogen, demonstrating high activities.[14] Thereafter, several alike *ansa*-aminoboranes (AABs) were studied in hydrogenation reactions. Among them, QCAT (Scheme 1) showed the best activity towards the hydrogenations of imines.[15]

Understanding the mechanistic aspects of catalytic transformation can play a crucial role in improving catalyst performance. In this respect, NMR spectroscopy offers a versatile toolbox to study reaction mechanisms. However, the detection of possible catalytic intermediates leading to product formation is usually not a trivial task, since highly active species are typically present in low concentrations that are hard to observe using conventional NMR methodology. This can become feasible if the sensitivity of the NMR methods is increased by means of nuclear spin hyperpolarization to boost

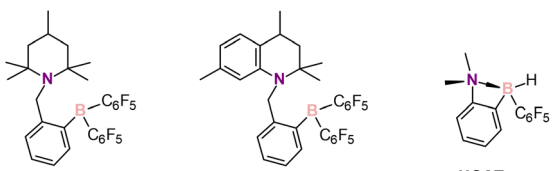

Scheme 1 Selected AABs used in hydrogenations with molecular hydrogen.

[a]*NMR Research Unit, Faculty of Science, University of Oulu, P.O. Box 3000, Oulu, 90014, Finland. E-mail: vladimir.zhivonitko@oulu.fi*
[b]*Department of Chemistry, University of Helsinki, A. I. Virtasen Aukio 1, 00014 Helsinki, Finland*

†Electronic supplementary information (ESI) available: Experimental procedures, NMR spectra, results of supplementary experiments. See DOI: https://doi.org/10.1039/d2dt02178a

‡Present address: Discovery, Product Development & Supply (DPDS), Janssen Pharmaceutical Companies of Johnson & Johnson, Turnhoutseweg 30, 2340 Beerse, Belgium.

signal intensities.[16] Parahydrogen-induced polarization (PHIP) is a specifically useful hyperpolarization technique in catalytic studies as hyperpolarization occurs naturally upon the chemical activation of H_2 molecules enriched in the para nuclear spin isomer.[17,18] When parahydrogen is activated by a catalyst, strongly enhanced NMR signals of the reaction intermediates or subsequent products can be observed, providing mechanistic information. To observe the hyperpolarization, H_2 activation must be pairwise, *i.e.*, the pair of H atoms must not be separated completely at least at the initial step.[19]

PHIP has demonstrated its power by proving the mechanisms of hydrogenation of various metal complex catalysts, especially in the detection of dihydride intermediates.[19,20] For example, it was used to study the kinetics of the formation of $[IrCO(H)_2I(PPh_3)_2]$ after the light-induced reductive elimination of hydrogen from that species;[21] to detect cationic Rh^I intermediates with coordinated arene rings;[22] to determine the pathways of H_2 exchange in $(\mu\text{-}H)_2Os_3(CO)_{10}$ clusters;[23] to understand ligand exchange in $[IrCO(H)_2Cl(PPh_3)_2]$ and $[IrH_2Cl(PPh_3)_3]$;[24] and in many other interesting mechanistic investigations[19,20,25] including heterogeneous catalytic systems.[26]

Although PHIP was mostly used to study reactions mediated by metal-containing catalysts,[19,20,27,28] it was reported that metal-free catalysts can activate parahydrogen, leading to PHIP effects.[29,30] Specifically, AABs were the first FLPs to show spin hyperpolarization effects in reactions with parahydrogen.[29,31,32] Later, several pnictogen biradicaloids were also documented as efficient metal-free parahydrogen activators.[33,34] Interactions of the discussed CAT and QCAT AABs with parahydrogen were shown to provide enhanced signals of NH and BH hydrogens of the corresponding CAT-H_2 and QCAT-H_2 adducts, respectively.[29] In general, until very recently, PHIP effects with metal-free compounds were observed exclusively for the catalyst–parahydrogen adducts formed at the initial H_2 activation step. In 2022, we reported the nuclear spin hyperpolarization of various alkenes achieved by alkyne hydrogenations with parahydrogen over a metal-free hydroborane catalyst HCAT (Scheme 1).[35]

Herein, we show that the metal-free AAB catalyst QCAT can hyperpolarize various amines in imine hydrogenations with parahydrogen, providing among other matters information about the hydrogenation catalytic process. We observed unusual one-hydrogen hyperpolarization of product amine NH protons in the ^{1}H NMR spectra. We demonstrate the reversibility of the catalytic cycle of imine hydrogenation catalyzed by QCAT *via* the observation of hyperpolarized amine when it was used as an individual initial reagent, shedding light on the mechanism of the involved catalytic transformations.

Results and discussion

Several aromatic imines were used to study hydrogenation with parahydrogen (Scheme 2). The reaction was performed at room temperature under 6 bar of 92% parahydrogen-enriched H_2, referred to as para-H_2 in the following text.

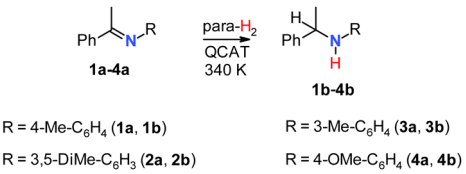

Scheme 2 The studied imine hydrogenations.

In the first experiments, the NMR spectra were recorded after introducing para-H_2 into solutions of QCAT (0.04 M) and imines (0.13 M) in toluene-d8, examining the reaction in a high magnetic field (9.4 T). Although imine structures have some influence on the observed hyperpolarization effects, the resulting ^{1}H NMR spectra generally demonstrated similar features. For instance, Fig. 1a illustrates the results of the hydrogenation of **1a** into **1b** with para-H_2 at 340 K. There are several signals that reveal the hyperpolarization effects *via* antiphase and negative in-phase multiplets. The four antiphase doublets centred at *ca.* 4.0 ppm correspond to the B–H group hydrogen of the QCAT-H_2 adduct; the splitting is induced by coupling to the spin-3/2 ^{11}B nucleus. The observation of antiphase signals is typical for high-field experiments according to the PASADENA experiment theory for weakly coupled spin-systems.[36] In contrast, the N–H group signal of QCAT-H_2 at *ca.*

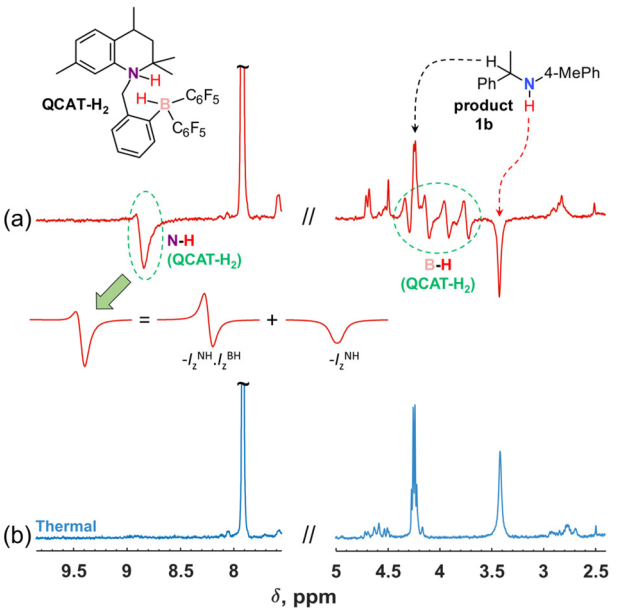

Fig. 1 ^{1}H NMR spectra of the QCAT-catalyzed hydrogenation of (1*E*)-*N*-(4-methylphenyl)-1-phenylethan-1-imine (**1a**) with para-H_2. The red spectrum (a) was acquired using a $\pi/4$ pulse just after introducing para-H_2 into a solution containing 0.04 M QCAT and 0.13 M of **1a** in toluene-d8 at 340 K. The enhanced antiphase signals correspond to the B–H group hydrogen (centred at 4.0 ppm) of the QCAT-H_2 adduct. The N–H group hydrogen of QCAT-H_2 (8.8 ppm) revealed a mixed antiphase/in-phase signal shape (see the decomposition). The N–H group hydrogen of amine product **1b** (3.4 ppm) revealed an enhanced in-phase negative signal. The blue spectrum (b) was recorded after the hyperpolarization relaxed at 340 K in 1 min, approaching the thermal equilibrium.

8.8 ppm shows a mixture of broad antiphase and in-phase negative signal contributions. The formation of the net negative polarization in the high-field experiment is unusual as coherent spin dynamics cannot lead to this effect.[35] However, it is crucial for the observation of the hyperpolarized amine **1b** as discussed below. As seen in Fig. 1a, the N–H group signal of the hydrogenation product **1b** appears as a negative in-phase signal at *ca.* 3.4 ppm (Fig. 1a), most likely inheriting the net negative polarization from the N–H hydrogen of QCAT-H_2.

Generally, the formation of a hyperpolarized QCAT-H_2 adduct is in accord with the proposed four-step mechanism of imine hydrogenations over QCAT (Scheme 3 and Scheme S1 in the ESI†).[15] According to this process, a hydrogen molecule is activated by QCAT, yielding the QCAT-H_2 adduct (Step **I**). The following proton transfer from the N–H group of QCAT-H_2 to the imine nitrogen atom results in an unstable ionic pair intermediate (Step **II**). The consequent hydride transfer from the anion to the cation leads to the dative QCAT-amine adduct (Step **III**). The last stage of the hydrogenation cycle releases the product amine and recovers the catalyst (Step **IV**). Either Step **II** or Step **IV** is the rate-determining step, depending on the substrate and catalyst structures.[15]

Importantly, Step **I** is pairwise and should lead to hyperpolarization after para-H_2 activation.[29] The formation of the final amine product **1b** *via* Steps **II**–**IV** either may or may not be pairwise, since the formation of the unlinked [QCAT-(B^-H) + imine-(N^+H)] ion pair at Step **II** can mix hydrogens coming from different para-H_2 molecules, preventing the pairwise H_2 transfer to form **1b** and observation of the antiphase contribution. In terms of magnetisation modes, this means that the two-spin order, $-I_z^{NH}\cdot I_z^{BH}$, inherited from para-H_2, must be destroyed by the non-pairwise process at Step **II**. In contrast, the single-spin net polarization, $-I_z^{NH}$, created by the QCAT-H_2 intermediate at Step **I**, can survive the non-pairwise transfer and result in hyperpolarized amine **1b**.

The non-pairwise nature of Step **II** can be confirmed to an extent indirectly. For instance, the hydrogenation of **1a** using borane catalyst $B(C_6F_5)_3$ does not lead to any hyperpolarization effects (see the ESI, Fig. S11†). In that case, the activation of para-H_2 is performed by an intermolecular borane–imine FLP, meaning that the intermolecular nature of FLPs prevents the observation of PHIP. A similar conclusion was drawn while comparing alkyne and alkene hydrogenations with intra- and intermolecular FLPs, respectively,[35] where the latter did not show any hyperpolarization effects but the former did (see the ESI, Fig. S13 and S14†). At the same time, we cannot rule out completely the possibility that the two-spin orders survived the chemical transformation because the *J*-coupling constant between the vicinal N–H and C–H protons in **1a** is small, which can lead to the mutual cancellation of the antiphase components.

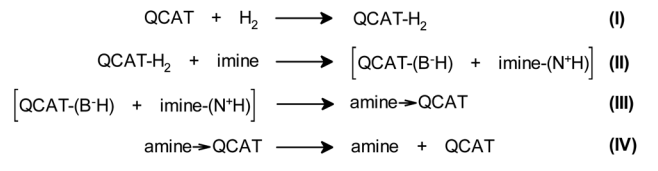

Scheme 3 Proposed mechanism of imine hydrogenation over the QCAT catalyst.

As we can be sure that the source of the negative net polarization of the N–H group proton in **1b** is the QCAT-H_2 intermediate, it is worth briefly discussing the reasons for its formation in Step **I**. There are examples of one-hydrogen polarization reported for metal complex catalysts, *e.g.*, in hydroformylation reactions (oneH-PHIP effect)[37] and the exchange of water ligands.[38] The observations were rationalized as a result of the para-H_2-derived protons exhibiting strong coupling in an intermediate, thus, accumulating net polarization *via* coherent dynamics before the transfer to the target substrate. However, in the case of QCAT-H_2, those protons are in the weak coupling regime ($\Delta\omega$ = 2 kHz at 9.4 T; J^{HH} = 3 Hz). In principle, the theory of the PASADENA effect in the case of weakly coupled systems predicts a negligible contribution to single-spin polarization, as kinetic averaging of the density operator leaves almost exclusively only $-I_z^{NH}\cdot I_z^{BH}$, when para-H_2 is added to highly magnetically inequivalent sites.[36] Moreover, knowing that the sign of the *J*-coupling constant is positive, the theory predicts positive possible single-spin polarization created by the coherent mixing on the N–H proton site in QCAT-H_2,[35,36] whereas our experiments show negative single-spin polarization. Most likely, the two-spin → single-spin-order transformation ($-I_z^{NH}\cdot I_z^{BH} \rightarrow -I_z^{NH}$) is induced by a cross-correlated relaxation process, *e.g.*, *via* correlated fluctuations of the dipole–dipole coupling of the N–H···H–B proton pair and the chemical shift anisotropy of the N–H proton in the QCAT-H_2 adduct.[39,40] This seems to be a common feature of the H_2 adducts of AABs, as similar effects have been observed and discussed in para-H_2 activations for a variety of such systems.[29,32,35] Indeed, a comparison of the hydrogenation of imine **1a** with para-H_2 in two different magnetic fields (9.4 and 14.1 T) revealed an increase in the net negative polarization level by a factor of 1.3–1.4 at the higher magnetic field for both QCAT-H_2 and the amine product **1b** (see Fig. S6 in ESI†). This observation indicates that the chemical shift anisotropy should indeed play an important role as its effect increases with the increase in the magnetic field strength. However, a more detailed discussion of this transformation requires extensive dedicated experiments that are beyond the scope of the current publication and will be done in the future. Experimental results on the hydrogenations of other imines (**2a**–**4a**) at 340 K are summarized in Fig. 2.

In all cases, the hyperpolarization effects were visible for para-H_2 originating hydrogens in the QCAT-H_2 intermediate and the N–H proton in amine products. The strengths of amine hyperpolarization, however, vary from one product to another. The in-phase negative signal of the N–H group hydrogen of **2b** observed *via* the hydrogenation of **2a** was slightly stronger as compared with that of **1b**. In principle, the use of more basic and more sterically hindered imines should lead to higher conversion rates,[15] and we could expect a somewhat higher intensity of the enhanced signal for **2b**. In the case of **3b**, the negative signal was not visible. Instead, the thermal

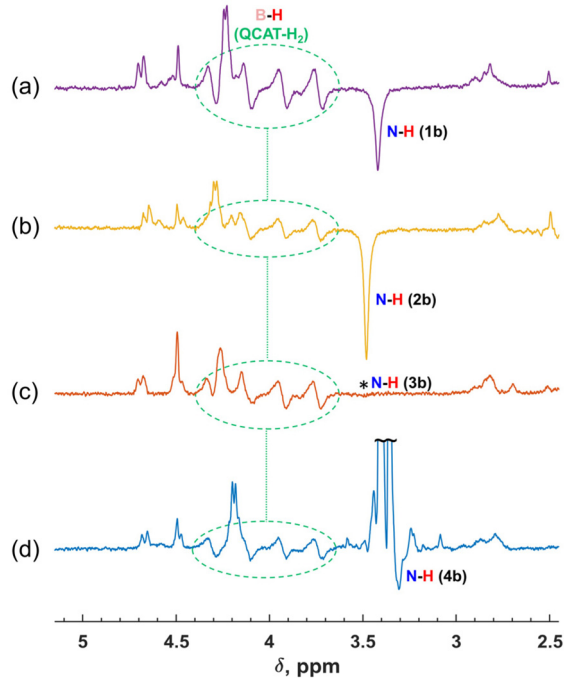

Fig. 2 (a)–(d) ^{1}H NMR spectra showing enhanced resonances observed in the hydrogenations of imines **1a–4a** with para-H_2 over the QCAT catalyst at 340 K in toluene-d8, respectively. The spectra were measured at the first moments after introducing para-H_2 into the corresponding imine–QCAT solutions. Spectral regions with the B–H group signals of the QCAT-H_2 intermediate and the N–H signals of the amine products **1b–4b** are displayed. Dotted ovals highlight the B–H group signals of QCAT-H_2. The positions of the amine products are shown with text labels. The position of the signal of the N–H group hydrogen of **3b** disappeared after introducing para-H_2, which is marked with an asterisk in (c).

signal of this amine disappeared after adding a fresh portion of para-H_2, implying the cancellation of the enhanced negative and thermal positive signals. The negative net polarization of the N–H group hydrogen was also observed in the case of **4b**, similarly to **1b** and **2b**. However, it was not that clearly visible due to the overlapping of the N–H and OCH_3 signals in the ^{1}H NMR spectra. Overall, the estimated signal enhancement factors due to hyperpolarization are 10 (**1b**), 15 (**2b**), 7 (**3b**) and 10 (**4b**) (see Table S1 in the ESI†), which are not record high values for PHIP. Theoretically, these factors can be more than four orders of magnitude for the ^{1}H nuclei in a 9.4 T magnetic field,[36] while the experimentally observed values are typically smaller but may be more than three orders of magnitude, *e.g.*, in hydrogenations of alkynes with para-H_2 using cationic Rh complexes as catalysts. Nevertheless, the rather moderate enhancements seen in our case still provided valuable qualitative information about the mechanistic features and consistency in the observed effects for different imine structures.

Further experiments showed that raising the temperature to 360 K can lead to the observation of a negative net polarization also for orthohydrogen (ortho-H_2; see the results for **1b** in Fig. S1 in the ESI†). Moreover, the C–H group hydrogen of the amine product revealed the hyperpolarization as well as the N–H group hydrogen. It was also visible that negative components of the B–H antiphase doublets of QCAT-H_2 become stronger than the positive ones. It seems that under these experimental conditions, the QCAT + H_2 ↔ QCAT-H_2 exchange is fast enough to release hyperpolarized free ortho-H_2 into the reaction "cocktail", which in turn is transferred into the amine product *via* Steps **I**–**IV**, contributing to the polarization of both C–H and N–H hydrogens. This observation pushed us to conclude that reversible exchange processes can play a significant role in the whole catalytic cycle at higher temperatures, allowing observation of the hyperpolarization effects when we substitute imine for amine as a substrate in the reaction mixture. In other words, we could expect to go through Steps **I**–**IV** in the reverse order and return, polarizing the amine substrate without alteration of its chemical structure. Indeed, when the experiments were repeated with QCAT, para-H_2 and commercial amine **1b** in the reaction mixture, the negative signal of the N–H group hydrogen of **1b** was observed at 360 K (Fig. 3a). The concentrations of the QCAT catalyst and amine were approximately on the same level as in the discussed imine hydrogenation reactions. We believe that these experiments show that basically all the mechanistic reaction steps shown in Scheme 3 must be reversible to a significant extent to enable the observation of the hyperpolarized amine without the formal hydrogenation of an unsaturated substrate.

The reverse Step **III** requires the abstraction of hydride from activated C(sp^3)–H bonds in primary or secondary amines. The feasibility of the abstraction was reported for strong Lewis acids, such as $B(C_6F_5)_3$.[41] For example, hydride abstraction from the activated α-position in NEt_2Ph proceeds in a facile

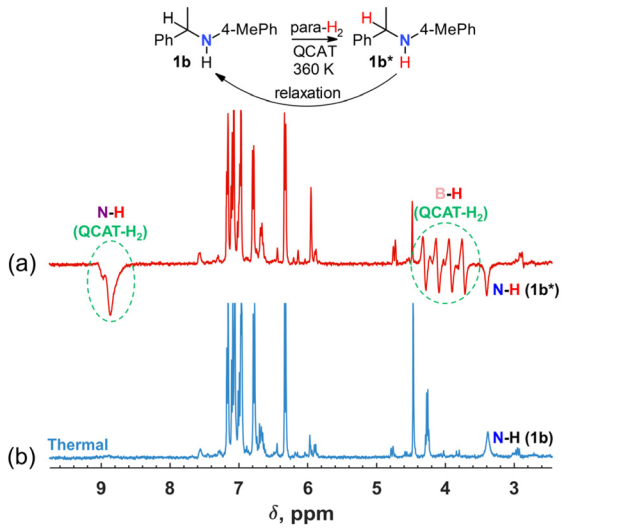

Fig. 3 ^{1}H NMR spectra acquired during the reaction of para-H_2, QCAT and **1b**. The red spectrum (a) was acquired using a π/4 pulse just after introducing para-H_2 into a solution containing 0.04 M QCAT and 0.04 M of **1b** in toluene-d8 at 360 K. The negative signal of the N–H proton of amine **1b** is clearly visible. The signal of the α-C–H hydrogen of **1b** completely vanished, indicating a weak hyperpolarization of this group. The blue spectrum (b) was recorded after relaxation to the thermal equilibrium.

manner to yield the corresponding iminium hydroborate. It can interact with the initial amine, deprotonating iminium with the formation of enamine and ammonium hydroborate salt.[41] A similar reversibility was also documented for the abstraction of α-C–H hydrogens in amines by QCAT. For instance, QCAT demonstrated a good racemization activity of amine **4b**,[15] which requires the elimination of α-hydrogen,[42] proving the ability of QCAT to dehydrogenate amines. The reversibility of Step **I** was known from previous studies.[29] In addition to this, our experiments show that Steps **II** and **IV** can be also reversible. The observed hyperpolarization effect of the reversible process was weaker as compared with that of the imine hydrogenation (see the N–H signals in Fig. 1a and 3a), but provided important mechanistic information. We also found in a test experiment an even weaker but still detectable hyperpolarization of the amino group in 1,2,3,4-tetrahydro-2,2,4,7-tetramethylquinoline, which does not have α-C–H hydrogen in the structure, in the exchange experiment at 360 K (Fig. S9 in the ESI†). This implies that the direct N–H···H–N exchange between QCAT-H_2 and the target amine may contribute to hyperpolarization. We should note that a similar proton transfer from the hyperpolarized QCAT-H_2 may serve as a route to sensitize other materials under exchange. This is the foundation of SABRE RELAY[43] and PHIP-X,[44] which obviously should be explored in future works with metal-free para-H_2 activators.

Finally, we tested the influence of QCAT concentration on the nuclear spin hyperpolarization effects. In addition to the described experiments with 33 mol% QCAT (Fig. 1 and 2), we conducted several reactions using lower catalyst loadings (see the ESI, Fig. S10†). The hydrogenation of imine **4a** with para-H_2 using 1–3 mol% of QCAT at 330 K did not lead to the observation of the enhanced antiphase and/or negative in-phase signals in the ^{1}H NMR spectra. Since the signals of QCAT-H_2 and the amine product **4b** were extensively hampered by the intense signals of the substrate, we were unable to see any hyperpolarization effects. The reaction rate also was significantly lower as compared with the high catalyst loading. In the experiment using 10 mol% QCAT, the rate significantly increased, and we observed hyperpolarization of the NH and BH hydrogens of QCAT-H_2 similarly to those with 33 mol% loadings. We noticed that the strength of these signals increased with the increase in the reaction temperature. The negative signal of the NH hydrogen of the amine product quite significantly overlapped with other signals in the spectrum in the case of **4b**.

Conclusions

Ansa-aminoboranes can provide interesting capabilities for hydrogenation catalysis without metals. Specifically, QCAT shows a relatively high activity in imine hydrogenations which can be tailored further to get even better results. Knowledge of the mechanistic details can extremely be helpful in this regard. In this study, we showed that parahydrogen-induced polarization can provide useful insights into the activation of H_2 by QCAT, proving the pairwise nature of this step. Moreover, using the single-spin negative net polarization created in QCAT-H_2 intermediates upon parahydrogen activation, it was possible to track the transfer of hydrogens to several imine substrates leading to the formation of hyperpolarized amine products. This is the first demonstration of the production of PHIP hyperpolarized amines from imines using metal-free catalysts. We also showed that when amines are used as initial substrates in the reaction with QCAT and parahydrogen their N–H group hydrogens can become hyperpolarized without any formal chemical structure changes, proving the reversibility of all the steps of the catalytic cycle. The variation in the catalyst concentration revealed the reaction rate alterations and the decrease in the amplitudes of the hyperpolarization effects at low catalyst loadings. An order of magnitude signal enhancements were observed for N–H hydrogen in amine products. We believe that further development of metal-free imine hydrogenation can lead to much higher enhancements, ideally reaching the levels of metal-containing catalysts. Generally, this study shows that PHIP-assisted mechanistic studies provide important mechanistic information about metal-free hydrogenations, as proved many times similarly for metal-containing catalysts[19,20,45,46] and, in addition to this study, only once for a metal-free catalyst.[35]

Author contributions

DOZ: investigation, validation, and writing – original draft; KC: conceptualisation, validation, and writing – review and editing; KS: validation and writing – review and editing; TR: conceptualisation, funding acquisition, resources, supervision, validation, and writing – review and editing; VVZ: conceptualisation, funding acquisition, resources, supervision, validation, visualisation, and writing – review and editing.

Conflicts of interest

There are no conflicts to declare.

Acknowledgements

This work was supported by the Academy of Finland (grant no. 323480) and the University of Oulu (Kvantum Institute). T. R. acknowledges the Academy of Finland for the financial support (grant no. 276586). The authors thank Dr Victor Sumerin (the University of Helsinki, former member) for the synthesis of the QCAT catalyst.

References

1 A. Kleemann and J. R. Engel, *Pharmaceutical Substances: Syntheses, Patents, Applications*, Thieme, Stuttgart, New York, 3rd edn, 1999.

2 A. Albert, *Selective Toxicity: The Physico-chemical Basis of Therapy*, Chapman and Hall, London, New York, 7th edn, 1985.
3 M. Beller and C. Bolm, *Transition Metals for Organic Synthesis: Building Blocks and Fine Chemicals*, Wiley-VCH, Weinheim, 2nd rev. and enl. edn, 2004.
4 C. E. Garrett and K. Prasad, *Adv. Synth. Catal.*, 2004, **346**, 889–900.
5 E. W. Baxter and A. B. Reitz, in *Organic Reactions*, 2002, vol. 59, pp. 1–714.
6 S. G. Ouellet, A. M. Walji and D. W. C. Macmillan, *Acc. Chem. Res.*, 2007, **40**, 1327–1339.
7 M. Rueping, E. Sugiono and F. R. Schoepke, *Synlett*, 2010, 852–865, DOI: **10.1055/s-0029-1219528**.
8 A. V. Malkov, K. Vrankova, S. Stoncius and P. Kocovsky, *J. Org. Chem.*, 2009, **74**, 5839–5849.
9 F. M. Gautier, S. Jones and S. J. Martin, *Org. Biomol. Chem.*, 2009, **7**, 229–231.
10 J. Seayad, A. Tillack, C. G. Hartung and M. Beller, *Adv. Synth. Catal.*, 2002, **344**, 795–813.
11 P. A. Chase, G. C. Welch, T. Jurca and D. W. Stephan, *Angew. Chem., Int. Ed.*, 2007, **46**, 8050–8053.
12 D. J. Chen and J. Klankermayer, *Chem. Commun.*, 2008, 2130–2131.
13 P. Spies, S. Schwendemann, S. Lange, G. Kehr, R. Frohlich and G. Erker, *Angew. Chem., Int. Ed.*, 2008, **47**, 7543–7546.
14 V. Sumerin, F. Schulz, M. Atsumi, C. Wang, M. Nieger, M. Leskelä, T. Repo, P. Pyykko and B. Rieger, *J. Am. Chem. Soc.*, 2008, **130**, 14117–14119.
15 V. Sumerin, K. Chernichenko, M. Nieger, M. Leskelä, B. Rieger and T. Repo, *Adv. Synth. Catal.*, 2011, **353**, 2093–2110.
16 J.-H. Ardenkjaer-Larsen, G. S. Boebinger, A. Comment, S. Duckett, A. S. Edison, F. Engelke, C. Griesinger, R. G. Griffin, C. Hilty, H. Maeda, G. Parigi, T. Prisner, E. Ravera, J. van Bentum, S. Vega, A. Webb, C. Luchinat, H. Schwalbe and L. Frydman, *Angew. Chem., Int. Ed.*, 2015, **54**, 9162–9185.
17 C. R. Bowers and D. P. Weitekamp, *Phys. Rev. Lett.*, 1986, **57**, 2645–2648.
18 C. R. Bowers and D. P. Weitekamp, *J. Am. Chem. Soc.*, 1987, **109**, 5541–5542.
19 B. J. Tickner and V. V. Zhivonitko, *Chem. Sci.*, 2022, **13**, 4670–4696.
20 S. B. Duckett and N. J. Wood, *Coord. Chem. Rev.*, 2008, **252**, 2278–2291.
21 B. Procacci, P. M. Aguiar, M. E. Halse, R. N. Perutz and S. B. Duckett, *Chem. Sci.*, 2016, **7**, 7087–7093.
22 R. Giernoth, P. Huebler and J. Bargon, *Angew. Chem., Int. Ed.*, 1998, **37**, 2473–2475.
23 S. Aime, W. Dastru, R. Gobetto, F. Reineri, A. Russo and A. Viale, *Organometallics*, 2001, **20**, 2924–2927.
24 C. J. Sleigh, S. B. Duckett and B. A. Messerle, *Chem. Commun.*, 1996, 2395–2396.
25 S. B. Duckett, in *Encyclopedia of Spectroscopy and Spectrometry*, ed. J. C. Lindon, G. E. Tranter and D. W. Koppenaal, Elsevier, Academic Press, 3rd edn, 2016, pp. 527–534.
26 K. V. Kovtunov, O. G. Salnikov, V. V. Zhivonitko, I. V. Skovpin, V. I. Bukhtiyarov and I. V. Koptyug, *Top. Catal.*, 2016, **59**, 1686–1699.
27 T. C. Eisenschmid, R. U. Kirss, P. P. Deutsch, S. I. Hommeltoft, R. Eisenberg, J. Bargon, R. G. Lawler and A. L. Balch, *J. Am. Chem. Soc.*, 1987, **109**, 8089–8091.
28 S. B. Duckett and C. J. Sleigh, *Prog. Nucl. Magn. Reson. Spectrosc.*, 1999, **34**, 71–92.
29 V. V. Zhivonitko, V.-V. Telkki, K. Chernichenko, T. Repo, M. Leskelä, V. Sumerin and I. V. Koptyug, *J. Am. Chem. Soc.*, 2014, **136**, 598–601.
30 L. E. Longobardi, C. A. Russell, M. Green, N. S. Townsend, K. Wang, A. J. Holmes, S. B. Duckett, J. E. McGrady and D. W. Stephan, *J. Am. Chem. Soc.*, 2014, **136**, 13453–13457.
31 V. V. Zhivonitko, K. Sorochkina, K. Chernichenko, B. Kotai, T. Foldes, I. Papai, V.-V. Telkki, T. Repo and I. Koptyug, *Phys. Chem. Chem. Phys.*, 2016, **18**, 27784–27795.
32 K. Sorochkina, V. V. Zhivonitko, K. Chernichenko, V. V. Telkki, T. Repo and I. V. Koptyug, *J. Phys. Chem. Lett.*, 2018, **9**, 903–907.
33 V. V. Zhivonitko, J. Bresien, A. Schulz and I. V. Koptyug, *Phys. Chem. Chem. Phys.*, 2019, **21**, 5890–5893.
34 V. V. Zhivonitko, H. Beer, D. O. Zakharov, J. Bresien and A. Schulz, *ChemPhysChem*, 2021, **22**, 813–817.
35 D. O. Zakharov, K. Chernichenko, K. Sorochkina, S. Yang, V. V. Telkki, T. Repo and V. V. Zhivonitko, *Chem. – Eur. J.*, 2022, **28**, e202103501.
36 C. R. Bowers, in *Encyclopedia of Nuclear Magnetic Resonance*, ed. D. M. Grant and R. K. Harris, Wiley, Chichester, 2002, vol. 9, pp. 750–769.
37 A. B. Permin and R. Eisenberg, *J. Am. Chem. Soc.*, 2002, **124**, 12406–12407.
38 M. Emondts, D. Schikowski, J. Klankermayer and P. P. M. Schleker, *ChemPhysChem*, 2018, **19**, 2614–2620.
39 A. Kumar, R. C. R. Grace and P. K. Madhu, *Prog. Nucl. Magn. Reson. Spectrosc.*, 2000, **37**, 191–319.
40 S. Aime, W. Dastru, R. Gobetto, A. Russo, A. Viale and D. Canet, *J. Phys. Chem. A*, 1999, **103**, 9702–9705.
41 J. Paradies, *Eur. J. Org. Chem.*, 2019, 283–294.
42 E. J. Ebbers, G. J. A. Ariaans, J. P. M. Houbiers, A. Bruggink and B. Zwanenburg, *Tetrahedron*, 1997, **53**, 9417–9476.
43 W. Iali, P. J. Rayner and S. B. Duckett, *Sci. Adv.*, 2018, **4**, eaao6250.
44 K. Them, F. Ellermann, A. N. Pravdivtsev, O. G. Salnikov, I. V. Skovpin, I. V. Koptyug, R. Herges and J.-B. Hövener, *J. Am. Chem. Soc.*, 2021, **143**, 13694–13700.
45 V. V. Zhivonitko, I. V. Skovpin, K. C. Szeto, M. Taoufik and I. V. Koptyug, *J. Phys. Chem. C*, 2018, **122**, 4891–4900.
46 V. V. Zhivonitko, I. V. Skovpin, M. Crespo-Quesada, L. Kiwi-Minsker and I. V. Koptyug, *J. Phys. Chem. C*, 2016, **120**, 4945–4953.